Published in final edited form as:

J Magn Reson Imaging. 2016 January ; 43(1): 88–98. doi:10.1002/jmri.24970.

Reliability of 7 Tesla 1H-MRS Measured Human Prefrontal Cortex Glutamate, Glutamine, and Glutathione Signals Using an Adapted Echo Time Optimised PRESS Sequence: A Between- and Within-Sessions Investigation

Níall Lally, MSc[#1,2,□], **Li An, PhD**[#3], **Dipavo Banerjee, BSc**[1], **Mark J. Niciu, MD**[1], **David A. Luckenbaugh, MA**[1], **Erica M. Richards, MD**[1], **Jonathan P Roiser, PhD**[2], **Jun Shen, PhD**[3], **Carlos A. Zarate Jr., MD**[1], and **Allison C. Nugent, PhD**[1]

[1]Experimental Therapeutics and Pathophysiology Branch, National Institute of Mental Health, National Institutes of Health, Bethesda, Maryland, USA

[2]Institute of Cognitive Neuroscience, University College London, Alexandra House, 17 Queen Square, London, WC1N 3AR, UK

[3]Magnetic Resonance Spectroscopy Core Facility, National Institute of Mental Health, National Institutes of Health, Bethesda, Maryland, USA

[#] These authors contributed equally to this work.

Abstract

Purpose—Evidence suggests that aberrant glutamatergic-signalling plays a role in numerous psychopathologies. To ascertain the mechanisms of neuropsychiatric illnesses and their treatment, accurate and reliable imaging techniques are required; proton magnetic resonance spectroscopy (^{1}H-MRS) can non-invasively measure glutamatergic function. Until recently, overlapping glutamatergic signals (glutamate, glutamine, and glutathione) could not easily be separated. However, the advent of novel pulse sequences and higher field magnetic resonance imaging (MRI) allows more precise resolution of overlapping glutamatergic signals, although the question of signal reliability remains undetermined.

Materials and Methods—At 7 T MR, we acquired ^{1}H-MRS data from the medial pregenual anterior cingulate cortex of healthy volunteers (N = 26) twice on two separate days. An adapted echo time optimised point resolved spectroscopy sequence, modified with the addition of a J-suppression pulse to attenuate N-acetyl-aspartate multiplet signals at 2.49 parts per million, was used to excite and acquire the spectra. In house software was used to model glutamate, glutamine, and glutathione, amongst other metabolites, referenced to creatine. Intraclass correlation coefficients (ICCs) were computed for within- and between-session measurements.

[□]Correspondence: Níall Lally, MD, 10 Center Drive, CRC, Room 7-5340, Bethesda, Maryland, 20892, Tel. (301) 402-9349; FAX (301) 402-9360, lallynm@mail.nih.gov.

Disclosures

A patent application for the use of ketamine in depression has been submitted listing Dr. Carlos A. Zarate Jr., M.D. among the inventors; he has assigned his rights on the patent to the U.S. government, but will share a percentage of any royalties that may be received by the government. All other authors have no conflicts of interest to disclose, financial or otherwise.

Results—Within-session measurements of glutamate, glutamine, and glutathione were on average reliable (ICCs ≥ 0.7). As anticipated, ICCs for between-session values of glutamate, glutamine, and glutathione were slightly lower but nevertheless reliable (ICC > 0.62). A negative correlation was observed between glutathione concentration and age ($r(24) = -0.37$; $P < .05$), and a gender effect was noted on glutamine and glutathione.

Conclusion—The adapted sequence provides good reliability to measure glutamate, glutamine and glutathione signals.

Keywords

Glutamatergic; intraclass correlation coefficient; point resolved spectroscopy; medial prefrontal cortex (mPFC); proton magnetic resonance spectroscopy; reliability

Introduction

The brain's glutamatergic system is fundamental to its function (1). Glutamate is the most abundant amino acid and principal excitatory neurotransmitter in the human brain (2). Glutamine, amongst other functions, is a precursor and principal metabolite of glutamate and is involved in the astrocytic cyclical regulation of glutamate (2). Glutathione, the most abundant brain anti-oxidant, provides a reservoir of neuronal glutamate (3) and serves important immunological roles. The tight regulation of these metabolites and neurotransmitters is a critical cornerstone of brain function (4). Proton magnetic resonance spectroscopy (^{1}H-MRS) provides a non-invasive estimate of these important neurochemicals. Indeed, studies using ^{1}H-MRS have linked abnormalities in the regulation of the glutamatergic system to numerous psychiatric and neurological disorders, including anxiety (5), major depressive disorder (MDD; (6–8)), Alzheimer's disease (9), and multiple sclerosis (10). Consistent with evidence of glutamatergic dysfunction in clinical populations, treatments that modify this system (11) have been reported to improve symptoms in some psychiatric conditions (12).

The potential for ^{1}H-MRS to help determine the mechanisms underpinning neuropsychiatric illnesses and their treatment remains both tantalising and tangible. However, to evaluate potential treatments using ^{1}H-MRS, its accuracy and reliability—both within- and between-sessions—must be determined (e.g. (13)). Scanner field strength is particularly important for accurately measuring glutamatergic signals using ^{1}H-MRS. A recently reported ^{1}HMRS sequence, evaluated at 7 T (14), affords enhanced detection of glutamate, glutamine, and glutathione. This sequence applies an extra excitation pulse to an echo time (TE) optimised point resolved spectroscopy (PRESS) sequence to weaken the contribution of the N-acetyl-aspartate (NAA) multiplet signal at 2.49 parts per million (ppm) via suppression of J-coupled NAA signals at 4.38 ppm; however, the reliability of this specific sequence (14) has yet to be quantified. Hence, the purpose of the present study was to assess the within- and between-session reliability of this specific sequence (other sequences have been evaluated at 7T; (13,15,16)) to detect neural glutamate, glutamine, and glutathione from a single medial prefrontal cortex voxel in healthy volunteers.

Materials and Methods

Participants

Twenty-six healthy volunteers (10 females and 16 males; mean age of all participants = 31.58 years, SD = 9.32, range = 20–54) were recruited to participate. Participants self-reported no history of head trauma, substance abuse or dependence, psychiatric or neurological illnesses. They were medically healthy as determined by physical and neurological examination and blood and urine laboratory tests. Psychiatric evaluation was performed by a specialist psychiatric nurse using the structured clinical interview for DSM-IV (17), and confirmed by a standard psychiatric interview by a board certified, practicing psychiatrist. The Combined Neuroscience Institutional Review Board at the NIH approved the study, and all participants provided written informed consent.

Design

Participants underwent MRI scanning once on two separate days (one session per day, each comprising two ^{1}H-MRS scans). The average time between each scanning session was 8.08 days (SD = 5.50, range = 2–21). Where possible, participants were scanned on the same day of the week and at the same time of day on the subsequent week or two weeks later.

MRI

All MRs were acquired using a Siemens 7 T MRI scanner. Images were collected using a 32-channel head coil. Standard 1 mm^3 isotropic resolution magnetization-prepared rapid gradient echo sequence images (repetition time (TR) = 3 s, TE = 3.9 ms, matrix = 256 × 256 × 256, inversion time (TI) = 1500 ms) were acquired on each of the two scanning days and used to create an anatomical brain image; this image was used to plan the location of the MRS voxel.

^{1}H-MRS

Using the anatomical image, a 2 × 2 × 2 cm^3 voxel was placed in the medial pregenual anterior cingulate cortex (pgACC; Fig. 1A). This region of the brain has been implicated in numerous neuropsychiatric disorders, particularly affective conditions such as major depressive disorder (MDD) (6,8,18), bipolar disorder (19,20), and generalized anxiety disorder (21). The region was localized by placing the midpoint of the voxel at the midline between the two hemispheres in the axial view and the edge of the voxel adjacent to the genu of the corpus callosum in the sagittal view, permitting maximal grey, and minimal white, matter concentration. To allow for consistency in voxel positioning between scanning sessions, a screenshot of the voxel placement on the first scanning day, comprising sagittal, axial and coronal voxel viewpoints (Fig. 1A), was created, and this was used to guide the second scanning session, which occurred on a different day. Voxel-specific first and second order B_0 shim coefficients were adjusted using a fast, automatic shimming technique by mapping along projections (FASTMAP;(22)) sequence. Next, a water FID (free induction decay) was acquired to calculate and correct for frequency drift, an important determinant of spectral quality (23). The B_1 field was optimized using a stimulated echo sequence consisting of $\alpha°$ - 90° - 90° - acquisition. The $\alpha°$ pulse has no localization gradient and the

two 90° pulses and acquisitions are localized. Hence, a one-dimensional bar going through the centre of the voxel was acquired and parameters were adjusted so that a null signal was found at the voxel centre. After these calibrations, water-suppressed MRS data were acquired using a TE-optimized PRESS pulse sequence modified by inserting a J-suppression pulse (14). Water suppression was accomplished using eight RF pulses of ~350 Hz bandwidth. The residual water signal amplitude was smaller than the NAA peak amplitude in most cases. Only one data set was excluded due to failed water suppression, a hardware issue, where the residual water signal amplitude was more than 10 times larger than the NAA peak amplitude.

The J-suppression pulse is a frequency-selective radiofrequency pulse placed at the resonance frequency of the aspartyl CH proton of N-acetyl-aspartate (NAA) at 4.38 ppm, thereby altering the J-evolution of the NAA aspartyl CH_2 multiplet at 2.49 ppm. The parameters TE_1 = 69 ms, TE_2 = 37 ms, and J-suppression pulse flip angle = 90° resulted in minimal NAA multiplet signals at 2.49 ppm while retaining near-maximum peak amplitudes for the C4 proton resonances of glutamate and glutamine using this sequence (14), and were thus used here. The J-suppression pulse combined with optimized TE values minimized the interference of the NAA multiplet signals at 2.49 ppm to the detection of the glutamine signals at 2.45 ppm and glutathione signals at 2.54 ppm, thus enhancing our ability to resolve these peaks. Other parameters for the modified PRESS sequence were: TR = 2.5 s, spectral width = 4000 Hz, number of data points = 2048 and number of transients = 128.

For each scanning session (two ^{1}H-MRS scans per session, one session per day), participants were inside the MRI scanner for approximately 100 minutes. ^{1}H-MRS data were acquired once following the acquisition of the anatomical image at the beginning and once again at the end of the session (note, there was only one scanning session on each day) following echo-planar imaging (EPI) functional MRI (to be reported elsewhere). Once the calibrations were complete, the total time for each ^{1}H-MRS scan was approximately six minutes. Due to the long gap between the first and second MRS scan (approximately one hour), when necessary, reshimming was undertaken for the second scan. Precisely the same procedure was repeated on the second scanning day.

^{1}H-MRS Modelling

The time-averaged 32-channel FID signals were merged into a combined single-channel metabolite FID using a generalized least squares method (24). The combined FID was Fourier transformed into the frequency domain to generate the spectrum, which was thereafter processed using a custom written linear combination fitting program to estimate metabolite levels. Basis sets included glutamate, glutamine, glutathione, γ-aminobutryic acid (GABA), NAA, N-acetylaspartylglutamate (NAAG), choline, and creatine. A Levenberg-Marquardt least square minimization algorithm was used in spectral fitting. The basis functions of the metabolites were scaled, apodized using a Voigt lineshape, frequency shifted, zero-order phase corrected, Fourier transformed to the frequency domain, and added with a spline baseline with eight control points to fit the spectral data between 1.8 and 3.3 ppm. Each metabolite could have different linewidth but was constrained to have the same Lorentzian/Gaussian ratio. The frequency of each metabolite was constrained to vary within

+− 6 Hz from its theoretical value. The zero-order phase of the spectral data was allowed to vary without any constraint. Metabolites were referenced to levels of creatine and are hereafter referred to by their metabolite names. Referencing to creatine reduces the need for tissue content correction because, similar to glutamatergic signals, creatine is only detected from the tissue and experiences the same blood-oxygen-level-dependent effects as other metabolites (25). NAA was summed with NAAG, henceforth known as total NAA (tNAA), for statistical analyses as the sequence used here is not optimal for reliable detection of NAAG (for an enhanced sequence to detect NAAG see (26)). The TE values used by this sequence suppressed GABA signals, and quantification of GABA was thus compromised. Cramér-Rao lower bounds (CRLB) expressions of parameter variance were computed (27). We computed the reduced chi-squared statistic for each spectrum to examine the fit of our model to the data; an arbitrary threshold of 12 or less for this statistic was set as an inclusion criterion for statistical analyses. Additionally, a water proton peak-line broadening criterion of 16 Hz was selected and only spectra with less than this value were included in the analyses.

Statistical Analyses

To rule out any systematic changes in our metabolites of interest (glutamate, glutamine, glutathione) we first assessed whether there was a main effect of scanning day or scan number, or an interaction between these two factors. We conducted a linear mixed model with compound symmetry selected as the covariance matrix and three fixed effects: scanning session (Day 1 or 2), scan number (1 or 2), and the interaction between these variables.

To determine the within- and between-session metabolite measurement reliability, we computed intraclass correlation coefficients in SPSS 21 (IBM SPSS, 2010, Chicago, IL, USA) with two-way random effects selected. Because we identified no effect for scan or day number on our metabolites of interest, we selected the more stringent absolute agreement (as opposed to consistency) option. We calculated reliability by comparing metabolites from the first and second scan (Scan 1 vs. Scan 2) within each day as well as the between-session reliability for each scan number (Day 1/Scan 1 vs. Day 2/Scan 1 and Day 1/Scan 2 vs. Day 2/Scan 2). The average (as opposed to single) measures ICC was selected from the SPSS output due to the averaging of both the FIDs and head coil channels conducted in the pre-processing stages. For consistency with previous neuroimaging studies (28), we used an ICC of 0.7 as our acceptable level. Specifically, poor, fair, good, and excellent reliability were arbitrarily defined as an average ICC value of < 0.6, $0.6 – 0.7$, $0.7 – 0.8$, and ≥ 0.8, respectively (29). Additionally, we computed the coefficient of variation (CV; calculated as the standard deviation of the mean difference between two data points, divided by the mean of the two data points) to make our assessment more comparable to other 7T reliability studies. For completeness, we also determined the ICCs, CVs and systematic variation for other metabolites quantifiable using our pulse sequence, namely, tNAA and choline. We also examined GABA to demonstrate that this sequence is not suitable for reliably detecting GABA. Because we used creatine as the reference for all metabolites, it was not possible to examine its reliability. The reliability quantification and assessment of systematic change for

tNAA, choline, and GABA was the same as for the analysis of glutamate, glutamine and glutathione.

We additionally assessed whether the number of days between each scanning day affected absolute change in any of our glutamatergic metabolites using Spearman's rho correlations due to the non-normal distribution. Finally, we also performed secondary exploratory analyses to examine previous reports of associations between our metabolites of interest and both gender and age. Higher glutamate levels (from a dorsolateral prefrontal cortex voxel) have been reported in men (30), and a negative correlation between age and glutamate (hippocampal and ACC) has also been found (31). We expected our enhanced sequence to provide excellent spectral resolution to examine the relative quantity of glutamate and glutamine and to confirm previously reported associations. Although no association between ^{1}H-MRS-measured glutathione and age has previously been reported, we predicted that such a relationship would exist because intracellular responses to redox intermediaries are known to be less efficacious with age (32). We also assessed possible gender effects related to ^{1}H-MRS-measured glutathione. These associations were assessed with linear mixed models with either gender or age entered as a fixed main effect and the dependent variable entered as glutamate, glutamine, or glutathione, averaged across scan number and day. Pearson product-moment correlations were used to assess the strength and direction of significant correlations. All statistical tests were two-tailed, with a significance threshold of $P < 0.05$.

Results

Some participants were missing at least one ^{1}H-MRS spectrum for the following reasons: withdrawal from the study before the second scanning day (n = 6 spectra); poor data quality (unsuppressed water linewidth > 16 Hz; n = 14 spectra); inability to acquire spectra due to scanner hardware, software or participant problems (n = 4 spectra); or our software's inability to accurately fit the data ($\chi^2 > 12$; n = 2 spectra). Thirteen participants had sufficient data quality for all four measurements. In total, there were 22 spectra for Day 1/Scan 1, 19 for Day 1/Scan 2, 20 for Day 2/Scan 1 and 17 for Day 2/Scan 2. The average water linewidth for all included spectra was 12.14 Hz (SD = 1.48), indicating high spectral resolution; a typical spectrum from one subject (Fig. 1B) and the corresponding model fit (Fig. 1C) is shown. Mean metabolite values (ratio to creatine) are presented in Table 1, and CRLB values are presented in Table 2.

No main effects were observed for Day, Scan, or their interaction on levels of glutamate (linear mixed models, $F_{(1,52)} = 0.29$, $P = 0.59$; $F_{(1,51)} = 1.06$, $P = 0.31$; $F_{(1,50)} = 0.11$, $P = 0.74$), glutamine (linear mixed models, $F_{(1,56)} = 0.36$, $P = 0.55$; $F_{(1,53)} = 1.26$, $P = 0.28$; $F_{(1,52)} = 0.03$, $P = 0.86$), glutathione (linear mixed models, $F_{(1,56)} = 0.08$, $P = 0.78$; $F_{(1,53)} = 0.07$, $P = 0.79$; $F_{(1,51)} = 0.15$, $P = 0.70$), GABA (linear mixed models, $F_{(1,61)} = 0.55$, $P = 0.46$; $F_{(1,56)} = 1.68$, $P = 0.20$; $F_{(1,54)} = 0.10$, $P = 0.75$), or tNAA (linear mixed models, $F_{(1,53)} = 0.61$, $P = 0.44$; $F_{(1,52)} = 0.02$, $P = 0.97$; $F_{(1,52)} = 0.44$, $P = 0.51$). Scan number significantly affected choline levels (linear mixed model, $F_{(1,51)} = 5.09$, $P = 0.03$), but scanning day did not, nor was there any effect from their interaction (linear mixed models,

$F_{(1,51)}$ = 0.74, P = 0.39; $F_{(1,51)}$ = 2.95, P = 0.09, respectively). The significant main effect of Scan number found for choline reflected lower levels for Scan 2 than Scan 1.

Time between the two scanning days did not significantly affect metabolite levels for glutamate (Spearman's rho, $r_{(19)}$ = 0.26, P = 0.28), glutamine (Spearman's rho, $r_{(19)}$ = 0.28, P = 0.25), or glutathione (Spearman's rho, $r_{(19)}$ = 0.31, P = 0.20).

As anticipated, ICC values for the within-session measures were higher than for the between-session measures for all metabolites (except glutathione, which was on average comparable both between- and within-sessions; Table 3). Bland-Altman plots depicting the four relationships (within scanning days 1 and 2 and between scan numbers 1 and 2) for each of our metabolites of interest are presented in Figure 2A–F. The corresponding CVs are also presented in Table 3. The reliability results obtained with our modified PRESS sequence may be summarized as follows. 1) On average, there was excellent within- (Fig. 2A) and between-session (Fig. 2B) reliability for glutamate. 2) Within-session reliability for glutamine was excellent (Fig. 2C), but between-session reliability was only fair (Fig. 2D). 3) Reliability for glutathione was on average fair within- and good between-sessions (Fig. 2E–F). 4) As expected, the reliability of GABA was poor (Table 3). 5) Reliability for tNAA and choline were excellent both within- and between-sessions (Fig. 3A–D). As choline was not a metabolite of interest per se, the more stringent absolute agreement ICC option was selected here despite the significant effect of scan number. CVs values were similar to ICCs with excellent reliability demonstrated using this statistic for glutamate, NAA and choline and fair-to-good reliability for glutamine and glutathione, both within- and between-session measurements (Table 3).

Finally, in our age- and gender-related analyses, we found a significant main effect of age on glutathione (linear mixed model, $F_{(15,\ 7)}$ = 3.47, P = 0.049), reflecting a negative correlation using the average across all scans (Pearson product-moment correlation, $r_{(24)}$ = −0.37), but no relationship between age and glutamate (linear mixed model, $F_{(15,\ 8)}$ = 1.58, P = 0.27) or glutamine levels (linear mixed model, $F_{(15,\ 8)}$ = 0.62, P = 0.80). In contrast to previous reports (30), there was no main effect of gender on glutamate (linear mixed model, $F_{(1,22)}$ = 0.29, P = 0.59). However, we found a significant effect of gender on glutamine (linear mixed model, $F_{(1,23)}$ = 8.55, P = 0.008) and glutathione (linear mixed model, $F_{(1,21)}$ = 4.32, P = 0.050); females had higher levels of glutathione, but lower levels of glutamine, than males.

Discussion

The present study used an adapted ^{1}H-MRS PRESS sequence (14) in a group of healthy volunteers and found that measures of medial pgACC glutamate, glutamine, and glutathione showed on average good-to-excellent within-session reliability and fair-to-excellent between-session reliability. The accurate and precise measurement of neurobiological substrates is critical to improving our understanding of the pathophysiology and treatment of neuropsychiatric disorders. Given that ^{1}H-MRS is the only non-invasive technique capable of measuring glutamatergic metabolites, it is important that its reproducibility be characterised.

Glutamate in particular, on average, showed excellent within- and between-session reproducibility, with high stability as evidenced by the low CRLB values. Corroborating the original report of this sequence (14), the high signal-to-noise ratio (SNR) for glutamate detection evident in our data likely arose from both the excellent separation afforded by the high-field MRI and the TE-optimized pulse sequence. The high reliability of glutamate measurements in healthy volunteers is promising with regard to the methodological approach presented here, and particularly important given the recent surge in interest in developing and evaluating glutamate-modulating pharmacological compounds for psychiatric and neurological conditions (33,34).

For glutamine, within-session reproducibility was excellent, but between-session reproducibility was only fair. Glutamine concentrations in the brain are much lower than those of glutamate (~40%, (35)), thus the SNR is poorer and the metabolite harder to resolve accurately; these factors make quantification errors more likely than with glutamate. Nevertheless, our methodological approach may still be robust enough to permit pharmacological investigation of glutamine-modulating agents; measurement of ^{1}H-MRS glutamine provides an important and distinct biological signal to glutamate. In a cyclical fashion, glutamate is enzymatically converted into glutamine by glutamine synthetase in astrocytes, where it is then transported back for subsequent reconversion to glutamate and packed into synaptic vesicles. Thus, ^{1}H-MRS measurement of glutamine may provide an index of astrocytic functioning relating to this particular cycle; the ratio of glutamine-to-glutamate may be particularly salient. Notably, alterations in glutamine (2) and astrocyte functionality (36) have been associated with a number of psychiatric conditions.

On average, pgACC glutathione levels showed fair reliability for within- and good for between-session measurements. Few studies have quantified neural glutathione with ^{1}H-MRS, as it is typically not resolvable at MRI scanner field strengths of 3 T or lower; however it is readily detectable at 7 T using sequences such as ours. Moreover, it remains an intriguing metabolite to explore clinically due to its functionality. Glutathione is the brain's primary antioxidant and is involved in inflammatory responses (37); indeed, aberrant ^{1}H-MRS glutathione concentrations have been found in several clinical conditions. For instance, Shungu and colleagues (37) found that depressed patients had significantly lower levels of occipital glutathione than healthy volunteers. Reductions in glutathione have also been observed in amyotrophic lateral sclerosis (38) and chronic fatigue syndrome (37), suggesting that ^{1}H-MRS glutathione levels may be an index of oxidative stress, which commonly occurs in psychiatric and neurological conditions. We also noted a decrease in glutathione with age, which is particularly interesting because ageing is associated with impaired immunity. Moreover, given the association between the glutathione redox system and age (32), it appears that ^{1}H-MRS-measured glutathione could be a sensitive marker of both cerebral ageing and immune function.

Our analyses suggest that tNAA and choline level measurements were also highly reliable, both within and between-sessions, using the sequence evaluated here. Given that these peaks are prominent within the standard ^{1}H-MRS spectrum, and are easily resolved at lower MRI field strengths, their high reliability here is reassuring and suggests that the reproducibility metrics for glutamate, glutamine and glutathione are appropriate. In contrast, the main effect

of scan number on choline levels was surprising; lower levels were observed for the second ^{1}H-MRS acquisition on each day. Because choline (2) is involved in cellular membrane turnover, this decrease may reflect decreased functional activity in this region.

At least three studies have examined within- or between-session reliability of ^{1}H-MRS at 7 T in healthy volunteers. Wijtenburg and colleagues (16) explored the between-session reliability of anterior cingulate cortex (ACC) and dorsolateral prefrontal cortex metabolites in a small sample (N = 4) using two distinct pulse sequences: STEAM and MEGA-PRESS-IVS. Both sequences demonstrated good measurement reliability, particularly for GABA. Stephenson and colleagues (15) assessed the between-session reproducibility of ACC and within- and between-session reliability of insula metabolites using STEAM, in 12 healthy males, and reported good reliability for both regions. Finally, Cai and associates (13) calculated the between-session (both same day and two weeks apart) reproducibility of their sequence in male volunteers at 7 T as an adjunct to a pharmacological investigation. They found that mean levels of occipital metabolites, collected separately using MEGA-PRESS and PRESS sequences, were similar (i.e. not statistically different) between scanning sessions, while drug administration significantly increased GABA levels. The CV values found here using our sequence are comparable, for both the between and within session measurements, to these first two investigations (15,16), with much less than 10% variation for glutamate, NAA and choline and on average, less than 15% for glutamine; Cai and colleagues do not report any reliability statistics. However, none of these three aforementioned reliability studies assessed the reproducibility of their metabolite quantification using typical reliability statistics, such as ICC, making precise comparisons between studies somewhat difficult. Moreover, none of the aforementioned studies reported metabolite values for glutathione, suggesting that the sequence used here is specifically able to estimate this important signal. Furthermore, the CRLBs observed here in our measurements and analyses are, on average, lower for all metabolites than for those reported using STEAM (16), suggesting that our sequence may offer enhanced sensitivity to detect most metabolites at 7 T.

Although the data presented here suggest that our methodological approach provides fair-to-excellent reliability for detecting glutamatergic metabolites and excellent spectral resolution in general, several limitations and asides should be acknowledged. First, some loss of data reproducibility may have occurred due to subject movement, partially arising from the long scan duration. Indeed, poor data (linewidth > 16 Hz) for a number of excluded spectra were likely due to subject movement; no methods exist to measure intra- and inter-^{1}H-MRS scan movement. However, our long scan time also reflects the realistic length of time required for intra-scanner drug administration studies. Second, the results presented here are specific to the modified pulse sequence and scanner strength used; it remains unknown whether different field strengths using our sequence would yield similar results. It is also unknown if another scanner of the same strength and brand using the same sequence would yield highly comparable results, as significant variation likely exists across MRI scanners and the precise hardware factors that influence ^{1}H-MRS measurement remain undetermined. Third, although 26 individuals participated in the study, our final dataset included many participants missing at least one data point. Future studies would benefit from a larger sample size and more complete scan set.

Several other factors should also be mentioned. First, our metabolites were referenced to creatine, which should fully afford tissue relative concentrations without the need for tissue correction; however, this remains to be tested empirically and appropriate concentration referencing remains a controversial topic. Indeed, Wijtenburg and colleagues (16) found a 12% variation of creatine between two scanning sessions, suggesting that creatine, or at least the measurement of this metabolite, may not be an appropriately reliable reference. Furthermore, referencing to creatine may not be applicable in comparisons between healthy volunteer and patient groups where creatine is potentially altered, for example in tumours; however, Maddock and Buonocore (2) note that consistent evidence for abnormal creatine levels in major psychiatric illnesses such as MDD or schizophrenia has not been found. Second, the gender effects noted for glutamine and glutathione are hard to explain. Some authors have suggested that gender differences in glutamatergic metabolites may result from differing neuroactive steroids (e.g. oestrogen, progesterone, and testosterone (30)). If these gender effects are replicated in a larger sample, then studies should incorporate strict between-group gender matching when appropriate. Third, several of our findings may actually be type 1 (false positive) errors, including the significant effect of scan timing on choline, the trend for glutamate, the effects of age and gender on glutathione, and the effects of gender on glutamine. Specifically, because these were exploratory analyses and numerous control tests were also completed, Bonferroni correction for multiple comparisons was not performed. Additionally, due to the low number of subjects and the lack of wide and systematic variation in age, these results remain tentative and require careful independent replication.

In conclusion, we used an adapted echo time optimised PRESS pulse sequence at 7 T to measure glutamate, glutamine and glutathione signals in the healthy human brain, and found that these measurements were on average reliable both within- and between-sessions. Taken together, our results suggest that 7 T ^{1}H-MRS is a useful tool for reliably measuring brain glutamate, glutamine and glutathione signals. If the promise of glutamatergic treatments for psychiatric and neurological conditions is realised, ^{1}H-MRS is well placed to play a pivotal role on the path towards understanding their mechanisms and advancing the progress of central nervous system therapeutics.

Acknowledgements

This work was funded in part by the Intramural Research Program of the National Institute of Mental Health, National Institutes of Health (IRP-NIMH-NIH; NCT00397111, protocol number 07-M-0021), by a NARSAD Independent Investigator to CAZ, and by a Brain & Behavior Mood Disorders Research Award to CAZ. The authors thank the 7SE research unit and staff for their support. Ioline Henter (NIMH) provided excellent editorial assistance.

Grant Support

This work was funded in part by the Intramural Research Program of the National Institute of Mental Health, National Institutes of Health (IRP-NIMH-NIH; NCT00397111, protocol number 07-M-0021), by a NARSAD Independent Investigator to CAZ, by a Brain & Behavior Mood Disorders Research Award to CAZ, and by a Wellcome Trust-National Institutes of Health joint PhD studentship (WT095465) to NL.

References

1. Magistretti PJ, Pellerin L. Cellular mechanisms of brain energy metabolism and their relevance to functional brain imaging. Philos Trans R Soc Lond B Biol Sci. 1999; 354(1387):1155–1163. [PubMed: 10466143]
2. Maddock, RJ.; Buonocore, MH. Curr Top Behav Neurosci. 2012. MR spectroscopic studies of the brain in psychiatric disorders; p. 11199-251.
3. Koga M, Serritella AV, Messmer MM, et al. Glutathione is a physiologic reservoir of neuronal glutamate. Biochem Biophys Res Commun. 2011; 409(4):596–602. [PubMed: 21539809]
4. Niciu MJ, Kelmendi B, Sanacora G. Overview of glutamatergic neurotransmission in the nervous system. Pharmacol Biochem Behav. 2012; 100(4):656–664. [PubMed: 21889952]
5. Pollack MH, Jensen JE, Simon NM, Kaufman RE, Renshaw PF. High-field MRS study of GABA, glutamate and glutamine in social anxiety disorder: response to treatment with levetiracetam. Prog Neuropsychopharmacol Biol Psychiatry. 2008; 32(3):739–743. [PubMed: 18206286]
6. Hasler G, van der Veen JW, Tumonis T, Meyers N, Shen J, Drevets WC. Reduced prefrontal glutamate/glutamine and gamma-aminobutyric acid levels in major depression determined using proton magnetic resonance spectroscopy. Arch Gen Psychiatry. 2007; 64(2):193–200. [PubMed: 17283286]
7. Lapidus KA, Gabbay V, Mao X, et al. In vivo (1)H MRS study of potential associations between glutathione, oxidative stress and anhedonia in major depressive disorder. Neurosci Lett. 2014:56974–79.
8. Walter M, Henning A, Grimm S, et al. The relationship between aberrant neuronal activation in the pregenual anterior cingulate, altered glutamatergic metabolism, and anhedonia in major depression. Arch Gen Psychiatry. 2009; 66(5):478–486. [PubMed: 19414707]
9. Fayed N, Modrego PJ, Rojas-Salinas G, Aguilar K. Brain glutamate levels are decreased in Alzheimer's disease: a magnetic resonance spectroscopy study. Am J Alzheimers Dis Other Demen. 2011; 26(6):450–456. [PubMed: 21921084]
10. Srinivasan R, Sailasuta N, Hurd R, Nelson S, Pelletier D. Evidence of elevated glutamate in multiple sclerosis using magnetic resonance spectroscopy at 3 T. Brain. 2005; 128(Pt 5):1016–1025. [PubMed: 15758036]
11. Stone JM, Dietrich C, Edden R, et al. Ketamine effects on brain GABA and glutamate levels with 1H-MRS: relationship to ketamine-induced psychopathology. Mol Psychiatry. 2012; 17(7):664–665. [PubMed: 22212598]
12. Dutta A, McKie S, Deakin JF. Ketamine and other potential glutamate antidepressants. Psychiatry Res. 2015; 225(1–2):1–13. [PubMed: 25467702]
13. Cai K, Nanga RP, Lamprou L, et al. The impact of gabapentin administration on brain GABA and glutamate concentrations: a 7T (1)H-MRS study. Neuropsychopharmacology. 2012; 37(13):2764–2771. [PubMed: 22871916]
14. An L, Li S, Murdoch JB, Araneta MF, Johnson C, Shen J. Detection of glutamate, glutamine, and glutathione by radiofrequency suppression and echo time optimization at 7 tesla. Magn Reson Med. 2015; 73(2):451–458. [PubMed: 24585452]
15. Stephenson MC, Gunner F, Napolitano A, et al. Applications of multi-nuclear magnetic resonance spectroscopy at 7T. World J Radiol. 2011; 3(4):105–113. [PubMed: 21532871]
16. Wijtenburg SA, Rowland LM, Edden RA, Barker PB. Reproducibility of brain spectroscopy at 7T using conventional localization and spectral editing techniques. J Magn Reson Imaging. 2013; 38(2):460–467. [PubMed: 23292856]
17. First, MB.; Spitzer, RL.; Gibbon, M.; Williams, JB. Biometrics Research. 2002. Structured Clinical Interview for DSM-IV-TR Axis I Disorders, Research Version, Patient Edition. (SCID-I/P).
18. Lally N, Nugent AC, Luckenbaugh DA, Niciu MJ, Roiser JP, Zarate CA Jr. Neural correlates of change in major depressive disorder anhedonia following open-label ketamine. J Psychopharmacol. 2015
19. Ellison-Wright I, Bullmore E. Anatomy of bipolar disorder and schizophrenia: a meta-analysis. Schizophr Res. 2010; 117(1):1–12. [PubMed: 20071149]

20. Lally N, Nugent AC, Luckenbaugh DA, Ameli R, Roiser JP, Zarate CA. Anti-anhedonic effect of ketamine and its neural correlates in treatment-resistant bipolar depression. Transl Psychiatry. 2014:4e469.
21. Etkin A, Prater KE, Hoeft F, Menon V, Schatzberg AF. Failure of anterior cingulate activation and connectivity with the amygdala during implicit regulation of emotional processing in generalized anxiety disorder. Am J Psychiatry. 2010; 167(5):545–554. [PubMed: 20123913]
22. Gruetter R. Automatic, localized in vivo adjustment of all first- and second-order shim coils. Magn Reson Med. 1993; 29(6):804–811. [PubMed: 8350724]
23. Near J, Edden R, Evans CJ, Paquin R, Harris A, Jezzard P. Frequency and phase drift correction of magnetic resonance spectroscopy data by spectral registration in the time domain. Magn Reson Med. 2014
24. An L, Willem van der Veen J, Li S, Thomasson DM, Shen J. Combination of multichannel single-voxel MRS signals using generalized least squares. J Magn Reson Imaging. 2013; 37(6):1445–1450. [PubMed: 23172656]
25. Lally N, Mullins PG, Roberts MV, Price D, Gruber T, Haenschel C. Glutamatergic correlates of gamma-band oscillatory activity during cognition: a concurrent ER-MRS and EEG study. Neuroimage. 2014; 85(Pt 2):823–833. [PubMed: 23891885]
26. An L, Li S, Wood ET, Reich DS, Shen J. N-acetyl-aspartyl-glutamate detection in the human brain at 7 Tesla by echo time optimization and improved Wiener filtering. Magn Reson Med. 2014; 72(4):903–912. [PubMed: 24243344]
27. Cavassila S, Deval S, Huegen C, van Ormondt D, Graveron-Demilly D. Cramer-Rao bound expressions for parametric estimation of overlapping peaks: influence of prior knowledge. J Magn Reson. 2000; 143(2):311–320. [PubMed: 10729257]
28. Nugent AC, Luckenbaugh DA, Wood SE, Bogers W, Zarate CA Jr. Drevets WC. Automated subcortical segmentation using FIRST: test-retest reliability, interscanner reliability, and comparison to manual segmentation. Hum Brain Mapp. 2013; 34(9):2313–2329. [PubMed: 22815187]
29. Brandt DJ, Sommer J, Krach S, et al. Test-Retest Reliability of fMRI Brain Activity during Memory Encoding. Front Psychiatry. 2013:4163.
30. O'Gorman RL, Michels L, Edden RA, Murdoch JB, Martin E. In vivo detection of GABA and glutamate with MEGA-PRESS: reproducibility and gender effects. J Magn Reson Imaging. 2011; 33(5):1262–1267. [PubMed: 21509888]
31. Schubert F, Gallinat J, Seifert F, Rinneberg H. Glutamate concentrations in human brain using single voxel proton magnetic resonance spectroscopy at 3 Tesla. Neuroimage. 2004; 21(4):1762–1771. [PubMed: 15050596]
32. Erden-Inal M, Sunal E, Kanbak G. Age-related changes in the glutathione redox system. Cell Biochem Funct. 2002; 20(1):61–66. [PubMed: 11835271]
33. Zarate C Jr. Machado-Vieira R, Henter I, Ibrahim L, Diazgranados N, Salvadore G. Glutamatergic modulators: the future of treating mood disorders? Harv Rev Psychiatry. 2010; 18(5):293–303. [PubMed: 20825266]
34. Kalia LV, Kalia SK, Salter MW. NMDA receptors in clinical neurology: excitatory times ahead. Lancet Neurol. 2008; 7(8):742–755. [PubMed: 18635022]
35. Govindaraju V, Young K, Maudsley AA. Proton NMR chemical shifts and coupling constants for brain metabolites. NMR Biomed. 2000; 13(3):129–153. [PubMed: 10861994]
36. Niciu MJ, Henter ID, Sanacora G, Zarate CA Jr. Glial abnormalities in substance use disorders and depression: does shared glutamatergic dysfunction contribute to comorbidity? World J Biol Psychiatry. 2014; 15(1):2–16. [PubMed: 24024876]
37. Shungu DC, Weiduschat N, Murrough JW, et al. Increased ventricular lactate in chronic fatigue syndrome. III. Relationships to cortical glutathione and clinical symptoms implicate oxidative stress in disorder pathophysiology. NMR Biomed. 2012; 25(9):1073–1087. [PubMed: 22281935]
38. Weiduschat N, Mao X, Hupf J, et al. Motor cortex glutathione deficit in ALS measured in vivo with the J-editing technique. Neurosci Lett. 2014:570102–107.

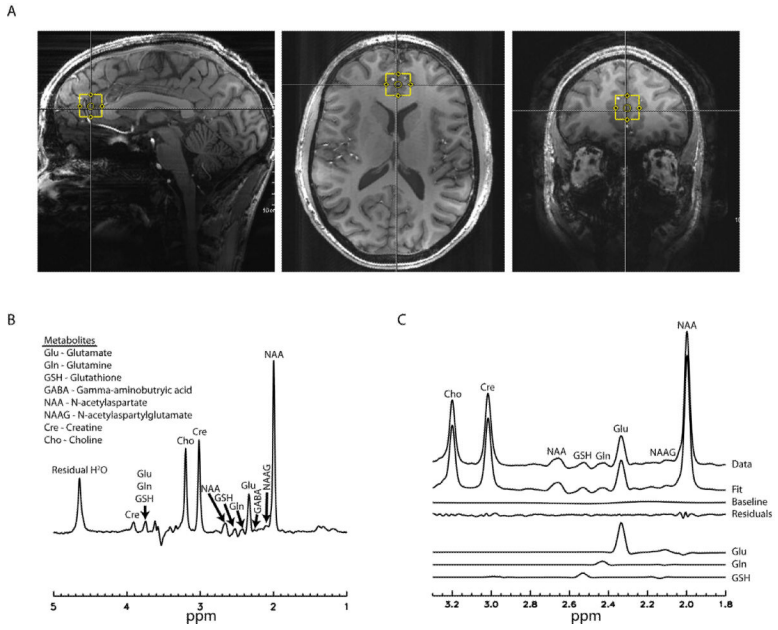

figure 1.

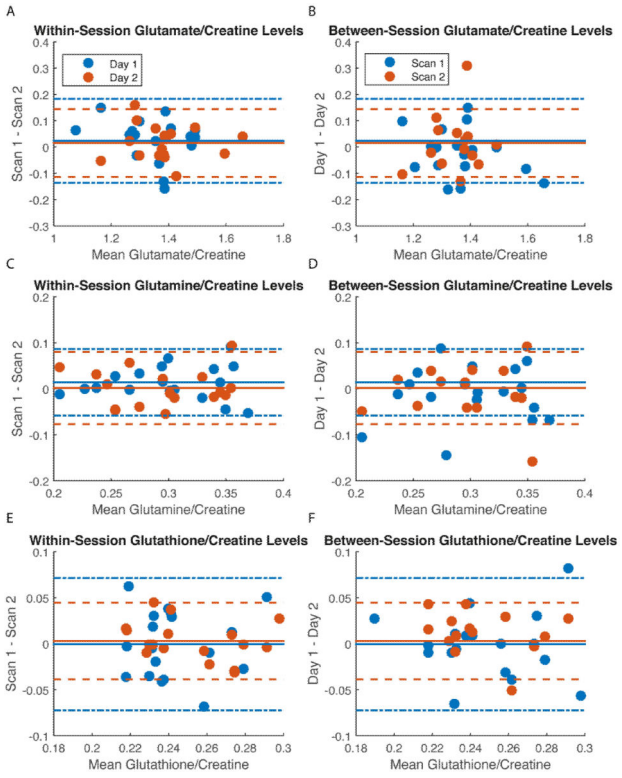

figure 2.

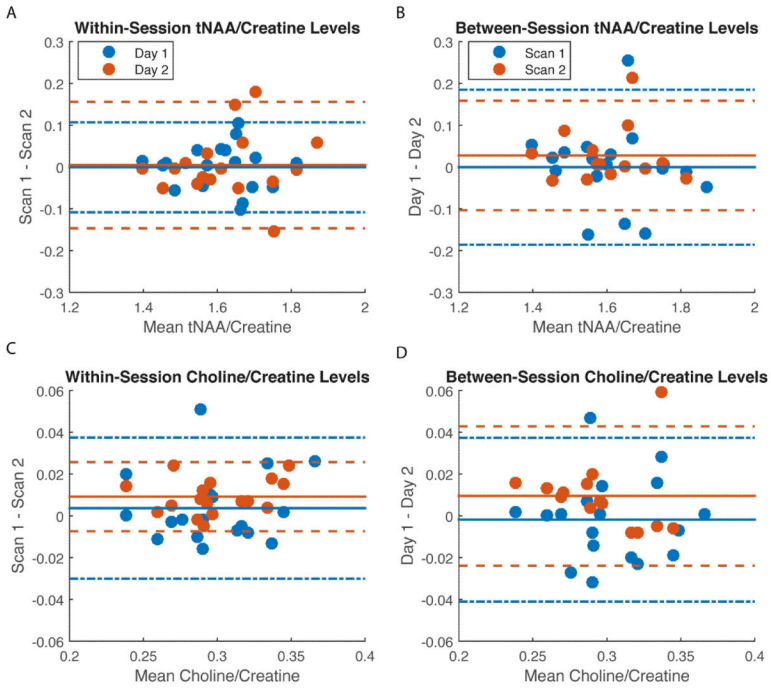

figure 3.

Table 1

Average raw metabolite means (standard deviations), relative to creatine, from each day and scan number.

Metabolite	Day 1/Scan 1	Day 1/Scan 2	Day 2/Scan 1	Day 2/Scan 2
Glu/Cre	1.37 (0.13)	1.33 (0.13)	1.38 (0.13)	1.38 (0.14)
Gln/Cre	0.30 (0.06)	0.29 (0.05)	0.30 (0.06)	0.29 (0.05)
GSH/Cre	0.25 (0.03)	0.24 (0.03)	0.25 (0.03)	0.25 (0.03)
GABA/Cre	0.20 (0.06)	0.19 (0.05)	0.20 (0.05)	0.18 (0.03)
tNAA/Cre	1.62 (0.12)	1.62 (0.11)	1.61 (0.14)	1.61 (0.14)
Cho/Cre	0.30 (0.04)	0.30 (0.04)	0.30 (0.03)	0.29 (0.03)

Abbreviations: Glu, glutamate; Gln, glutamine; GSH, glutathione; GABA, γ-aminobutyric acid; tNAA, total N-acetyl-aspartate; Cho, choline Cre, creatine.

Table 2

Average metabolite percentage CRLB (standard deviations) for each metabolite.

Metabolite	Day 1/Scan 1	Day 1/Scan 2	Day 2/Scan 1	Day 2/Scan 2
Glu	1.58 (0.40)	1.54 (0.27)	1.47 (0.38)	1.35 (0.20)
Gln	6.76 (2.20)	6.86 (1.78)	6.16 (1.74)	5.90 (0.96)
GSH	6.14 (1.20)	6.13 (1.38)	5.83 (2.25)	5.35 (0.82)
GABA	6.69 (2.93)	6.39 (1.57)	5.99 (1.95)	5.89 (1.10)
NAA	0.76 (0.32)	0.69 (0.18)	0.71 (0.27)	0.64 (0.18)
NAAG	6.03 (3.42)	5.73 (3.93)	6.07 (4.54)	4.33 (1.24)
Cre	0.76 (0.23)	0.76 (0.18)	0.72 (0.23)	0.66 (0.18)
Cho	0.92 (0.29)	0.91 (0.22)	0.85 (0.30)	0.79 (0.19)

Abbreviations: CRLB, Craméer-Rao Lower Bound; Glu, glutamate; Gln, glutamine; GSH, glutathione; GABA, γ-aminobutyric acid; NAA, *N*-acetyl-aspartate; NAAG, *N*-acetylaspartylglutamate; Cre, Creatine; Cho, choline.

Table 3

Intraclass correlation coefficient and coefficient of variation (CV, %) values between-and within-scanning sessions.

Metabolites	Within Day 1 (Scan 1 vs. Scan 2; n = 18)		Within Day 2 (Scan 1 vs. Scan 2; n = 17)		Between-Session (Scan 1; n = 18)		Between-Session (Scan 2; n = 14)	
	ICC	CV	ICC	CV	ICC	CV	ICC	CV
Glu/Cre	0.88	6.00	0.94	4.77	0.86	6.48	0.68	7.95
Gln/Cre	0.87	12.44	0.84	13.40	0.63	15.53	0.62	9.38
GSH/Cre	0.49	14.95	0.88	8.54	0.65	11.45	0.76	8.25
GABA/Cre	−0.17	36.89	0.37	29.19	−0.26	30.92	0.21	15.43
tNAA/Cre	0.94	3.38	0.93	4.79	0.88	4.60	0.90	2.09
Cho/Cre	0.94	5.77	0.97	2.82	0.93	4.75	0.91	3.39

Abbreviations: ICC, intraclass correlation coefficient; CV, coefficient of variation; Glu, glutamate; Cre, creatine; Gln, glutamine; GSH, glutathione; GABA, γ-aminobutyric acid; tNAA, total *N*-acetyl-aspartate; Cho, choline.